J Porous Mater (2016) 23:1311–1318
DOI 10.1007/s10934-016-0190-3

Sonophotocatalytic degradation of eriochrome black-T dye in water using Ti grafted SBA-15

Heba M. Gobara[1] · Radwa A. Elsalamony[1] · Salah A. Hassan[2]

Published online: 1 June 2016

Abstract Here in, a series of titanium-modified mesoporous silica (Ti-SBA-15) was prepared by grafting titanium isopropoxide. The as-synthesized Ti-SBA-15 nanocatalysts were characterized through N_2-adsorption–desorption, XRD, TGA/DSC, TEM and EDX techniques. Sonocatalytic and sonophoto-catalytic degradation of Eriochrome Black T (EBT) dye were investigated. 88.7 % removal was achieved in 70 min by using 5 % Ti-SBA-15 through sonophotocatalytic degradation under visible light irradiation. The kinetic study revealed that photo-degradation of EBT follows pseudo-first order reaction mechanism, where the rate constant was 27.4×10^{-3} min^{-1}.

Keywords SBA-15 · Titanium isopropoxide · Grafting · Sonophotocatalysis · Eriochrome black-T

1 Introduction

It is well known that through textile industry, a great deal of dyes and pigments used are lost and released in the wastewater effluents. Such highly polluted streams have become a serious environmental problem. The efforts have continued along the last two decades to remove dyes from effluent water streams through several approaches, such as adsorption, ultra-filtration, reverse osmosis, coagulation [1–3], biodegradation [4], chlorination, ozonation [5], etc. On the other hand, the advanced oxidation processes (AOPs), based on generation of very reactive species (e.g., hydroxyl radicals, ·OH), capable of oxidizing a broad range of pollutants, have been improved during the last decade to eliminate the problem of dye destruction in aqueous systems. A variety of AOPs processes, including Fenton and photo-Fenton catalytic reactions [6, 7], H_2O_2/UV processes [8, 9], TiO_2 mediated photocatalysis [10–12], sonolysis and sonophotocatalysis [13–16] has been applied for this aim, at a wide range of operational conditions.

TiO_2 has been conventionally used as a nontoxic photocatalyst due to its low cost, high catalytic activity and photostability [1]. During photoexcitation at $\lambda \leq 380$ nm, absorption of a photon by TiO_2 promotes an electron into the conduction band (CB), generating an electron–hole pair. The conduction band electron is available for reduction and the valence band (VB) hole is available for oxidation. In condensed oxygenated aqueous media, the completely hydroxylated surface of TiO_2 generates upon photoexcitation hydroxyl radicals, in an adsorbed state, as powerful oxidizing agents.

Alternatively, ultrasonic irradiation of aqueous solutions can result in the growth and collapse of gas bubbles (cavitation), producing higher transient temperatures and pressures which leads to the formation of free radicals via the homolysis of water:

$$H_2O \xrightarrow{\text{Ultrasound}} H + OH.$$

Ultrasonic irradiation has been demonstrated as a promise approach for the purification of contaminated water (or textile effluents), where hydroxyl radical mediated chain oxidation processes were involved [17, 18].

In view of the addressed approaches in the literature, the aim of the present study was focused on conjugating the

✉ Heba M. Gobara
hebagobara@yahoo.com

[1] Egyptian Petroleum Research Institute, 1 Ahmed El-Zomor St., Nasr City, Cairo 11727, Egypt

[2] Chemistry Department, Faculty of Science, Ain Shams University, Abbassia, Cairo 11566, Egypt

use of a newly developed flexible nanostructured TiO_2 of efficient visible photocatalytic activity with applying ultrasonic irradiation for removal of mono-azo textile Eriochrome Black T dye in aqueous solutions. This is the so called sonophotocatalytic removal process.

Several researchers have endeavored to incorporate TiO_2 into high surface area composite systems. Among these systems, TiO_2–SiO_2 composites have been widely used in various industrial and environmental applications [2–4].

Ordered mesoporous silicas have been developed during the last two decades, where various mesoporous structures were roughly classified into three categories based on the pore shape: nearly spherical cage, cylindrical channel and bi-continuous channel [11–14]. The SBA-type (Santa Barbara Amorphous) is the most frequently studied ordered mesoporous silica. For instance, SBA-15 silica exhibits interesting textural properties, such as large specific surface area, uniform-sized pores, thick framework walls, small crystallite size of primary particles, high surface-to-volume ratio and high thermal stability [19–21]. Ti-SBA-15 was synthesized by incipient wetness impregnation [21] or by grafting in hexane [22], either directly by using microwave heating [19] or in the presence of fluoride ion additive [20]. The direct synthesis of Ti-SBA-15 was not recommended as only a limited ratio of titanium was allowed to be incorporated in the composite framework under the strongly acidic conditions [23].

In the present work, an ordered mesoporous composite was synthesized, with a homogenous layer of TiO_2 in the mesopore system of SBA-15, through graphting of Ti-isopropoxide on SBA-15. Sonophotocatalytic approach was applied for removal of mono-azo textile Eriochrome Black T dye in aqueous solution, by using Ti-SBA-15 catalysts (of 2.5 and 10 % Ti content) under visible light illumination accompanied with ultrasonication. For comparison purposes, a sonocatalytic approach was also applied for the removal process, only by using ultrasound agitation without illumination.

2 Experimental

2.1 Synthesis of SBA-15 and Ti—SBA-15 graphated samples

The SBA-15 material was synthesized according to [24], using Pluronic P123 triblock copolymer (PEG-PPG-PEG) as a structure directing agent and tetraethyl orthosilicate (TEOS) as a silica source. In a typical synthesis, 4 g of Pluronic P123 was dissolved under stirring in water and 2 M HCl. The required amount of TEOS (Aldrich) was added at 35 °C and the mixture was kept under stirring for 20 h for aging. The pH of solution was controlled at ~ 1, to enhance the formation of ordered hexagonal SBA-15 with uniform pores up to 30 nm, and the mixture was subsequently aged at 80 °C overnight. The obtained solid was then filtered, washed thoroughly with deionized water and dried in air at room temperature. The calcination was carried out by slowly increasing the temperature from room temperature to 500 °C in 8 h (with a heating ramp = 1 °C).

Ti-SBA-15 composite samples (with 2.5 and 5 % Ti content) were prepared via grafting of titanium isopropoxide. For this purpose, a desired amount of titanium (IV) isopropoxide (Ti/Si = 2.5, 5 %) was dispersed in 150 ml of dry isopropyl alcohol (99.7 %, Merck) and mixed with 4 g of SBA-15 under vigorous stirring for 3 h at ambient temperature. The solid was filtered, washed with isopropyl alcohol and dried overnight at ambient temperature. Finally, the titanium-grafted samples were calcined at 550° C for 4 h.

2.2 Physicochemical characterization

N_2 adsorption–desorption isotherms at −196 °C were determined by the aid of a NOVA 3200 apparatus, USA. The samples were previously out gassed under a reduced pressure at 200° C for 4 h. Specific surface areas (S_{BET}) were calculated from multi-point isotherms at relative pressure (P/P_o) ranging from 0.05 to 0.30. Pore size distribution curves were obtained by Barrett, Joyner and Halenda (BJH) method using the adsorption branch of the isotherms.

The powder X-ray diffraction (XRD) patterns were recorded adopting a Brucker D8 advance X-ray diffractometer, using Cu–Kα radiation ($\lambda = 1.5418$ Å) with 30 mA and 40 kV in the 2θ from 10° to 80° range with a scan rate of 10° min^{-1}. DSC-TGA analyses were carried out for the catalyst samples using simultaneous DSC-TGA SDTQ 600, USA under N_2 atmosphere, with a heating rate of 10 °C min^{-1}. The morphology of the samples was investigated by the aid of high contrast transmission electron microscope model JEOL TEM-1230 (Japan), 120 K, with magnification as high as 600,000, attached with (EDX)-Oxford X-Max.

2.3 Sonocatalytic and photocatalytic removal procedure of Eriochrome Black (EB) T dye (BT)

The Eriochrome Black T dye (BT) azo dye supplied by Aldrich had the following characteristics: C.I. number 14645; formula weight 461.38 g/mol; λmax = 410 nm.

A schematic illustration of the experimental set-up is shown in Scheme 1. It consists of an ultrasonic homogenizer (VCX-750, Sonic and materials, Inc.), equipped with

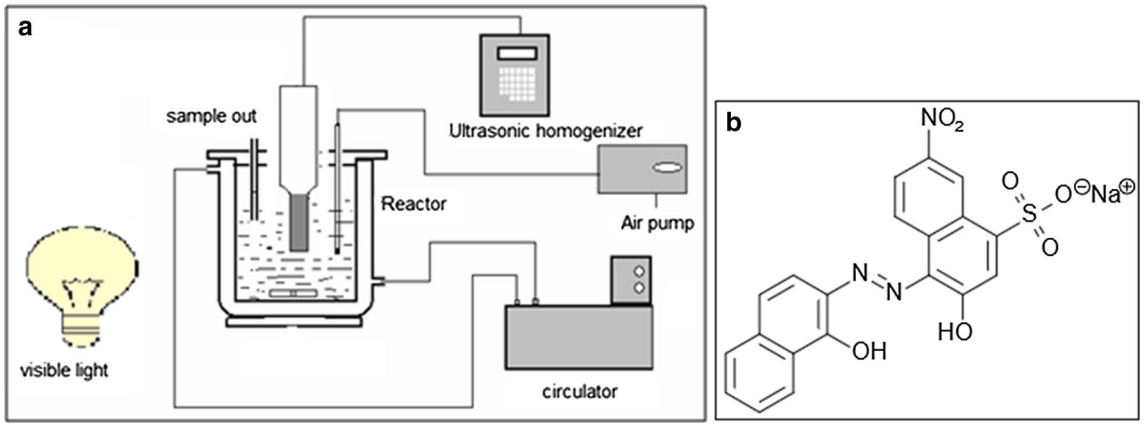

Scheme 1 **a** Experimental set-up for dye sonocatalytic and sonophotocatalytic removal and **b** Chemical structure of Eriochrome Black T dye (Sodium 1-[1-Hydroxy naphthylazo]-6-nitro-2-naphthol-4-sulfonate

a titanium probe (of diameter 13 mm) operating in a continuous mode at a fixed frequency of 20 kHz with adjusted electric output power at 125 W for 20 min. A 200 W tungsten lamp of visible light ($\lambda > 400$ nm) was used as the irradiation source. Air was blown into the reaction medium by an air pump in a constant flow to maintain the solution saturated with oxygen during the course of the reaction. The experiments were carried out in a glass reaction vessel containing 300 ml dye solution of 50 ppm concentration and a catalyst weight of 0.3 g at 25 ± 1 °C [25, 26]. In sonocatalytic removal runs, only ultrasound agitation was used without illumination. For sonophotocatalytic runs, visible light irradiation was applied together with ultra-sonication. Suspensions of 10 ml were withdrawn at regular intervals and immediately filtrated to completely remove the catalyst particles. For following up the progress of dye removal, the changes in concentrations were monitored using UV/VIS spectrophotometer (JENWAY-6505 UV–visible spectrophotometer) at $\lambda_{max} = 410$ nm. Before sonocatalytic and sonophotocatalytic experiments, the possible photolysis and sonolysis of EBT dye were investigated. The aqueous solution of the dye was exposed solely to ultrasound or visible lamp irradiation and the change of dye concentration was followed up. Neither photolysis nor sonolysis was occurred in the studied processes (Scheme 1).

3 Results and discussions

3.1 Surface identification of SBA-15 and Ti/SBA-15 catalyst

The obtained N_2 adsorption–desorption isotherms and pore size distribution curves determined by BJH method for parent SBA-15 and Ti-SBA-15 catalyst samples are illustrated in Fig. 1a. The derived surface parameters of such samples are summarized in Table 1. The obtained isotherms for all samples are of type IV according to IUPAC classification [27], characterizing ordered mesoporous materials. These isotherms exhibit H1 hysteresis loops, related most probably to uniform cylindrical pores of relatively larger dimensions, arisen originally from the SBA-15 material. Moreover, the pronounced steep in adsorption branches of the isotherms favors a narrow pore size distribution, which is typical of the well-ordered mesoporous structures, as depicted in Fig. 1b. It is clearly evident from Table 1 that, the specific surface area (S_{BET}) as well as the pore dimensions (total pore volume, V_p and average pore radius, r_p) decrease considerably by incorporating Ti into SBA-15 matrix. The recorded surface parameters continue to decrease gradually by increasing the Ti ratio, due most probably the inclusion of Ti atoms into the SBA-15 pore system [28]. These findings are further confirmed from pore size distribution (PSD) profiles shown in Fig. 1b. All the PSD curves show unimodal distribution, where the most abundant hydraulic pore radius is shown to decrease gradually from 42.7 Å for the parent SBA-15–27.9 Å for 5 % Ti- SBA-15 sample of narrower mesoporous system (Table 1). Guided by EDX analysis, it may be concluded that only ~50 mol% of the applied Ti is incorporated into the Ti-SBA-15 matrix, mainly in the pore system, during the grafting process, in both the 2.5 % Ti-SBA-15 and 5 % Ti-SBA-15 catalyst samples [29].

3.2 XRD analysis

Figure 2 illustrates the XRD patterns of parent SBA-15 and different synthesized Ti-SBA-15 samples in both low angle and high angle regions. It is evidently clear that all samples under study exhibit a broad diffraction band at 2θ of 15-35°, related almost to their amorphous nature. No

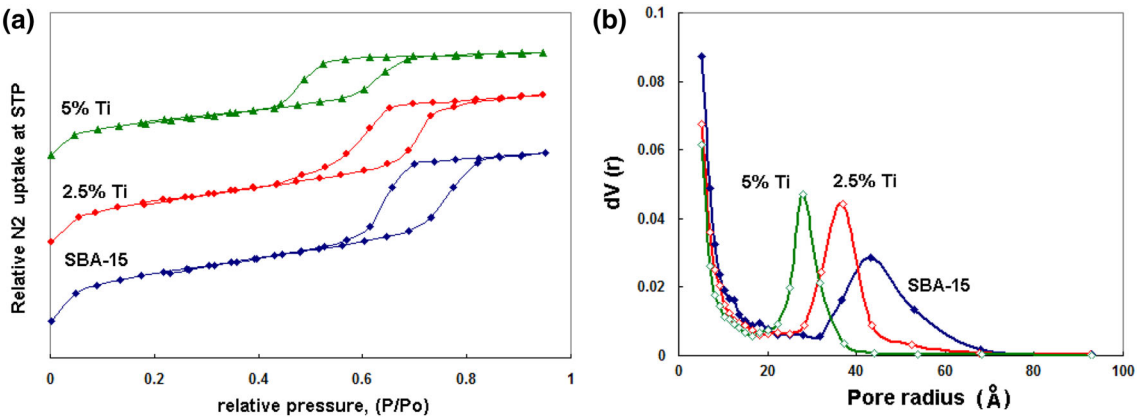

Fig. 1 N_2 adsorption desorption **a** and Pore size distribution *curve* **b** of SBA-15 and Ti grafted SBA-15 catalysts

Table 1 Surface parameters of SBA-15 and Ti-SBA-15 catalyst samples

Catalyst	S_{BET}(m^2/g)	V_p (cm^3/g)	r_p (Å)	(Ti/Ti + Si)[a] (mol%)
SBA-15	804.4	0.918	43.2	–
2.5 % Ti-SBA-15	674.9	0.793	36.8	2.5
5 % Ti-SBA-15	607.3	0.596	27.9	5.1

[a] From EDX data

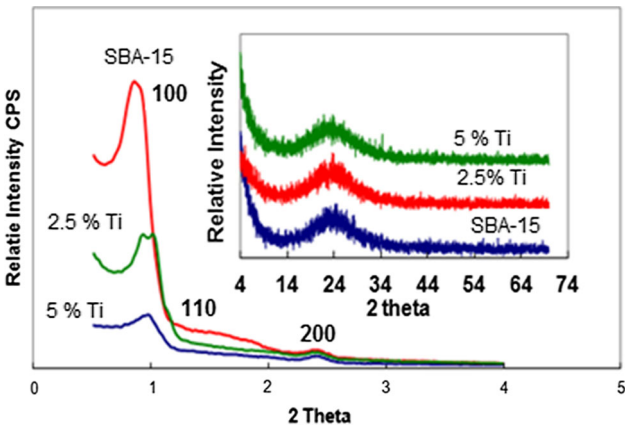

Fig. 2 Low-angle XRD patterns of parent SBA-15 and Ti-SBA-15 catalyst samples of (Ti/Si = 2.5 and 5 %) and (*inset*) high-angle XRD patterns of SBA-15 and Ti-SBA-15 samples

diffraction lines characterizing SiO_2 or TiO_2 phases could be detected [27, 28], indicating that both these phases seem to exist in amorphous states. Moreover, the complete absence of crystalline domains of titanium oxide, as rutile or anatase phase, may be linked with their too small crystallite sizes hardly detectable by X-ray diffraction or the tiatania component may be segregated as an amorphous phase within the silica matrix.

On the other hand, the intense signals in the low angle region represent a diffraction pattern characteristic of the p6 mm symmetry of the hexagonal array of pores in the SBA-15 [22, 26, 30–32]. The presence of three well resolved reflections, corresponding to the 100, 110 and 200 symmetries may refer to the mesoporous structure. The 100 reflection observed at almost the same 2θ values for the titania-grafted samples may suggest that the incorporation of Titania into silica matrix does not affect the interplanar spacing of the SBA-15 structure [15, 16].

3.3 Thermal analysis

The TGA/DSC analyses of SBA-15 and Ti-graphted catalysts under N_2 atmosphere are represented in Fig. 3. Almost the same thermal trend seems to be displayed in all samples, exhibiting only one endothermic peak at T max = 65 °C, accompanied with a weight loss of 8.0 %, related most likely to the removal of the physically adsorbed water (Fig. 3a). By incorporating Ti into SBA-15 structure, this endothermic peak is shifted toward a higher temperature (namely, T max = 80–90 °C), associated with 9.1 and 11.0 % weight losses for 2.5 and 5 % Ti, respectively. A shallow endothermic peak relevant to the removal of the chemisorbed water molecules or hydroxyl groups at temperatures between 200 and 400 °C was also detected by the DSC. This peak was in practical accompanied by a weight loss of 2 wt%, according to Fig. 3b [33]. The total losses of weight at the end of the test were 12.8, 12.9 and 13.6 % for parent SBA-15, 2.5 % Ti-SBA-15 and 5 % Ti-SBA-15, respectively. This trend is extremely insured the

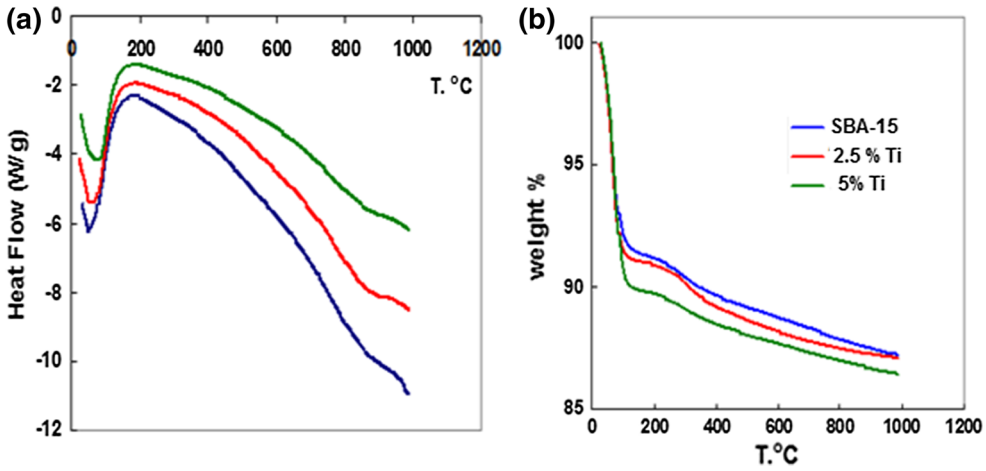

Fig. 3 DSC (**a**) and TGA (**b**) *curves* of SBA-15 and Ti/SBA-15 catalysts with different Ti loadings: 2.5 % Ti and 5 % Ti

high thermal stability of the used catalysts up to 1000 °C [34].

3.4 TEM investigation

The TE-Micrographs of SBA-15 and Ti-SBA-15 catalyst samples are shown Fig. 4. The original SBA-15 micrograph (a) reveals sets of hexagonally well-ordered mesoporous channels running along the length of the particles. The micrographs of Ti-SBA-15 samples (2.5 and 5 % Ti) show dense black spots, related to Titania nanostructure, located at the external surface of SBA-15. These spots become denser with the increase of Ti %, confirming the successful grafting of Ti species as an intense homogenous layer on the surface of ordered mesoporous SBA-15 (micrographs b and c).

As no strong characteristic peaks of crystalline TiO_2 appeared in the XRD patterns, elemental analysis by EDX is performed in this study to quantify percentages by weight of different elements in a catalyst sample. The amount of energy emitted depends on the type of atom present in the sample; hence each atom will have a characteristic peak in the EDX spectrum with a height corresponding to its concentration. The results of the attached EDX analysis for both catalyst samples are recorded in Fig. 5. TiO_2 seems to be completely incorporated into the SBA structure, according to the relative concentrations applied, with almost homogeneously distributed layer onto the various silica particles. The relative percentage of titania appears to be increased for 5 % Ti–Si sample at the expense of silica percentage present in the sample, i.e., in an obvious interaction profile. Very close average global percentages of Ti and Si are observed at several sample zones, with only a scattering of $\sim \pm$ 15 %. Small EDX peaks between 8 and 10 eV are referred to residual Cl ion from the HCl acid medium used.

3.5 Sonocatalytic and Sonophotocatalytic activities of Eriochrome Black T (EBT) dye

In this work, removal of Eriochrome Black T (EBT) dye was studied through sonocatalysis, i.e., by using ultrasound agitation only without illumination or through sonophotocatalysis, i.e., by applying visible irradiation together with ultra-sonication. The changes in dye concentration were monitored using UV/VIS spectrophotometer at

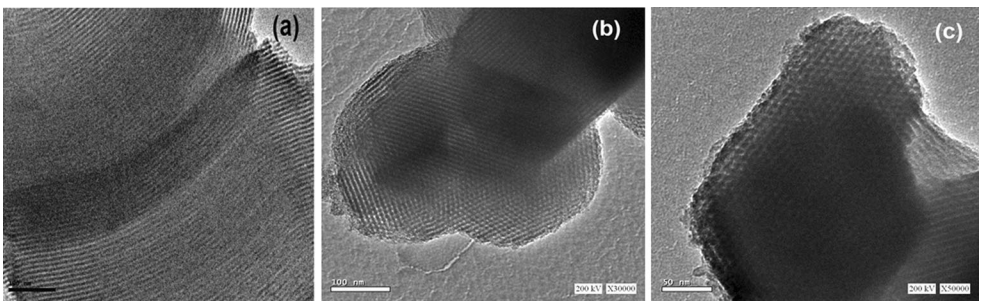

Fig. 4 HR-TEM micrographs of **a** SBA-15 and Ti/SBA-15 catalysts with different Ti loadings: **b** 2.5 % Ti and **c** 5 % Ti

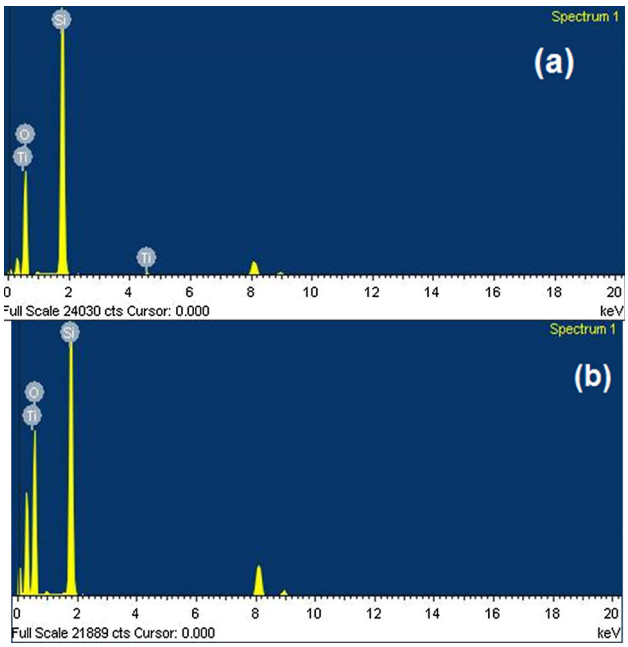

Fig. 5 The EDX measured composition of Ti-SBA-15 catalysts of: **a** 2.5 % Ti and **b** 5 % Ti

$\lambda_{max} = 410$ nm. Neither photolysis nor sonolysis occurred in the studied processes.

The dye removal efficiencies of the SBA-15, 2.5 % Ti/SBA-15 and 5 % Ti/SBA-15 samples after sonocatalysis and sonophotocatalysis are depicted in Fig. 6. It is evident that sonophoto- catalysis demonstrates superior dye degradation ability, compared to sonocatalysis [35–37]. In both cases, the dye removal % shows an increase with the exposure duration. Marked increase in removal % and removal rate is observed by incorporation of increased ratio of Ti in SBA-15 matrix. The 5 % Ti/SBA-15 sample is ensured to have the highest activity, achieving 88.7 % removal after 70 min long sonophotocatalysis. Analysis of removal data reveals the validity of pseudo-first order kinetics on all the catalyst samples under study, confirming the superiority of the sonophotocatalysis.

Analysis of removal data reveals the validity of pseudo-first order kinetics on all the catalyst samples under study, confirming the superiority of the sonophotocatalysis [37–39]. The kinetic parameters derived from the pseudo-first order plots are listed in Table 2, which indicate the marked increase in the removal rate constant (*k*) by increasing the Ti content in the sample. The higher regression coefficients (R^2), ensuring also the validity of pseudo-first order model, run in harmony with the (*k*) values being the highest for the 5 % T-SBA-15.

In an attempt to interpret the prevailing effect of sonophotocatalysis, it is worth mentioning that sonophotocatalysis relies on two types of irradiation: visible and ultrasonic. When a surface of TiO_2 nanoparticles is irradiated with light energy equal to or larger than its band gap energy ($E \geq 3.2$ eV), conduction band electrons (e^-_{cb}) and valence band holes (h^+_{vb}) are generated [36, 38]. The formed photo-excited electrons and holes can either recombine or react with surrounding molecules. These electron–hole pairs react with molecules such as H_2O and O_2, producing very reactive radicals (viz., $OH^{\cdot}$, O_2^{-}) that are responsible for the dye degradation. In addition to these reactions, dye degradation may also take place directly by oxidation with holes or reduction with electrons. In our studied cases, the aqueous solution of dye undergoes in the same time an ultrasonic irradiation through creation of acoustic cavitations [36, 37]. Thus, the newly formed micro bubbles grow and subsequently collapse leading to a generation of extremely high local temperatures and pressure rise [40]. Under such extreme conditions, the primarily formed hydroxyl ($OH^{\cdot}$) and hydrogen ($H^{\cdot}$) radicals are most likely followed by generation of oxidizing hydroperoxyl radicals ($HO_2^{\cdot}$) and hydrogen peroxide species. The excessive concentrations of these reactive species may be

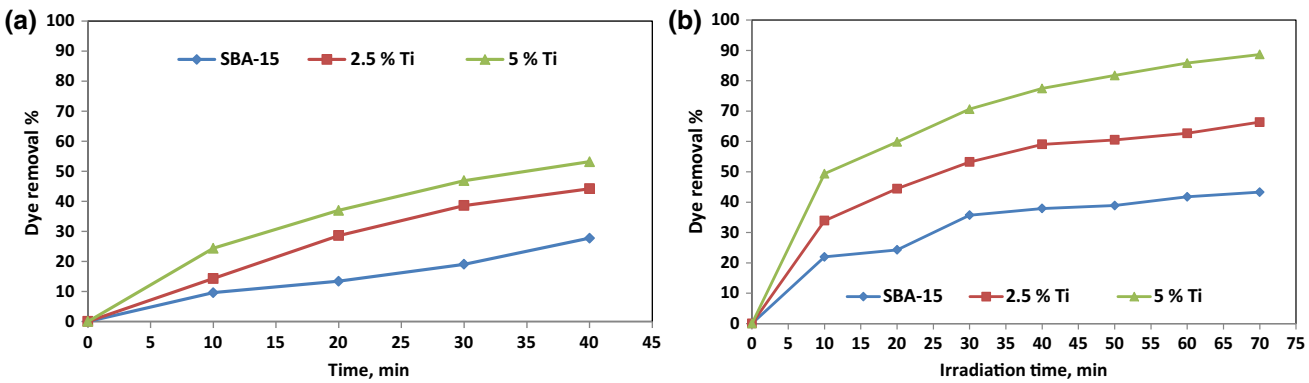

Fig. 6 EBT dye removal from the aqueous solution by **a** sonocatalysis and **b** sonophotocatalysis in the presence of SBA-15, 2.5 % Ti/SBA-15 and 5 % Ti/SBA-15 samples

Table 2 The pseudo-first rate constants of EBT dye degradation in the presence of SBA-15, 2.5 % Ti/SBA-15 and 5 % Ti/SBA-15 samples

Samples	Sonocatalysis		Sonophotocatalysis	
	$k \times 10^{-3}$, min^{-1}	R^2	$k \times 10^{-3}$, min^{-1}	R^2
SBA-15	7.4	0.9554	8.5	0.9123
2.5 %Ti-SBA-15	14.4	0.9818	16.1	0.9963
5 % Ti-SBA-15	16.1	0.9936	27.4	0.9971

in favor of the applicability of sonophotocatalysis, than the sonocatalysis or photocatalysis solely [41].

4 Conclusion

SBA-15 ordered mesoporous materials and Ti grafted SBA-15 catalysts (with 2.5 and 5 % Ti content) were successfully synthesized. Several characterization techniques were adopted such as N_2-adsorption–desorption, XRD, TGA/DSC, TEM and EDX. Sonocatalytic and sonophoto-catalytic degradation of Eriochrome Black T (EBT) dye were investigated to the first time over these kinds of catalysts. The results revealed that the synthesized catalysts are thermally stable up to 1000° C. No diffraction lines characterizing SiO_2 or TiO_2 phases could be detected in XRD patterns indicating that both silica and titania phases seem to exist in amorphous states. The textural properties by TEM ensured the formation of hexagonally well-ordered mesoporous SBA-15 channels running along the length of the particles. Ti-SBA-15 samples showed dense black spots, related to titania nanostructure, located at the external surface of SBA-15. These spots became denser with the increase of Ti %, confirming the successful grafting of Ti species as an intense homogenous layer on the surface of ordered mesoporous SBA-15. The photocatalytic activity of these synthesized catalysts was tested for eriochrome black T degradation under visible light irradiation through sonocatalysis or sonophotocatalysis. Among the catalysts tested, the 5 % Ti/SBA-15 sample had the highest activity, achieving 88.7 % removal after 70 min long sonophotocatalysis. Analysis of removal data revealed the validity of pseudo-first order kinetics on all the catalyst samples under study, confirming the superiority of the sonophotocatalysis.

References

1. C.T. Kresge, M.E. Leonowicz, W.J. Roth, J.C. Vartuli, J.S. Beck, Nature **359**, 710 (1992)
2. J.S. Beck, J.C. Vartuli, W.J. Roth, M.E. Leonowicz, C.T. Kresge, K.D. Schmitt, C.T.W. Chu, D.H. Olson, E.W. Sheppard, S.B. McCullen, J.B. Higgins, J.L.J. Schlenker, Am. Chem. Soc. **114**, 10834 (1992)
3. A. Sayari, Chem. Mater. **8**, 1840 (1996)
4. A. Corma, Chem. Rev. **97**, 2373 (1997)
5. T. Maschmeyer, F. Rey, G. Sanker, J.M. Thomas, Nature **378**, 159 (1995)
6. A. Corma, V. Fornés, M.T. Navarro, J. Pérez-Pariente, J. Catal. **148**, 569 (1994)
7. T. Blasco, A. Corma, M.T. Navarro, J. Pérez-Pariente, J. Catal. **156**, 65 (1995)
8. K.A. Koyano, T. Tatsumi, Microporous Mater. **10**, 259 (1997)
9. R. Mokoya, W. Jones, Chem. Commun. **22**, 2185 (1997)
10. R. Ryoo, S.J. Jun, J.M. Kim, M.J. Kim, Chem. Commun. **22**, 2225 (1997)
11. J.Y. Ying, C.P. Mehnert, M.S. Wong, Angew. Chem. Int. Ed. **38**, 56 (1999)
12. F. Schüth, Chem. Mater. **13**, 3184 (2001)
13. Y. Wan, D.Y. Zhao, Chem. Rev. **107**, 2821 (2007)
14. Y. Han, D. Zhang, Curr. Opin. Chem. Eng. **1**, 129 (2012)
15. W.J.J. Stevens, K. Lebeau, M. Mertens, G. van Tendeloo, P. Cool, E.F. Vansant, J. Phys. Chem. B **110**, 9183 (2006)
16. F. Zhang, Y. Yan, H. Yang, Y. Meng, C. Yu, B. Tu, D. Zhao, J. Phys. Chem. **109**, 8723 (2005)
17. W. Zhang, J. Lu, B. Han, M. Li, J. Xiu, P. Ying, C. Li, Chem. Mater. **14**, 3413 (2002)
18. Z. Luan, E.M. Maes, P.A.W. van der Heide, D. Zhao, R.S. Czernuszewicz, L. Kevan, Chem. Mater. **11**, 3680 (1999)
19. N. Rahmat, A.A. Zuhairi, A. Rahman Mohamed, Am. J. Appl. Sci. **7**, 1579 (2010)
20. R. Huirache-Acuña, R. Nava, C.L. Peza-Ledesma, J. Lara-Romero, G. Alonso-Núñez, B. Pawelec, E.M. Rivera-Muñoz, Materials **6**, 4139 (2013)
21. B.L. Newalkar, J. Olanrewaju, S. Komarneni, Chem. Mater. **13**, 552 (2001)
22. M.S. Morey, S. O'Brien, S. Schwarz, G.D. Stucky, Chem. Mater. **12**, 898 (2002)
23. P. Wu, T. Tatsumi, T. Komatsu, T. Yashima, Chem. Mater. **14**, 1657 (2002)
24. D. Zhao, J. Sun, Q. Li, G.D. Stucky, Chem. Mater. **12**, 275 (2000)
25. A.K. Aboul-Gheit, S.M. Abdel-Hamid, S.A. Mahmoud, R.A. El-Salamony, J. Valyon, M.R. Mihályi, A. Szegedi, J. Mater. Sci. **46**, 3319 (2011)
26. H. Gobara, R. El-Salamony, D. Mohamed, M. Mishrif, Y. Moustafa, T. Gendy, Chem. Mater. Res. **6**(6), 63–81 (2014)
27. S.A. Mahmoud, H.M. Gobara, Synthesis of nanostructured mesoporous ordered silica supported Fe_2O_3 nanoparticles for water purification, "Processing of nanostructure materials and nanostructure films",ed. By Kathy Lu, Chris Li, Eugene Medvedoveski and Eugene A. Olevesky, Ceramics Transaction Volume 233, the American Chemical Society, Wiley (2010)
28. M.-J. Kim, S.-H. Chang, J.-S. Choi, W.-S. Ahn, React. Kinet. Catal. Lett. **82**(1), 27 (2004)
29. K.S.W. Sing, D.H. Everett, R.A.W. Haul, L. Moscou, R.A. Pierotti, Pure Appl. Chem. **57**, 603 (1985)
30. K. Chandra Mouli, K. Soni, A. Dalai, J. Adjaye, Appl. Catal. A Gen. **404**, 21 (2011)

31. G. Muthu Kumaran, S. Garg, K. Soni, M. Kumar, L.D. Sharma, G. Murali Dhar, K.S. Rama Rao, Appl. Catal. A Gen. **305**, 123 (2006)
32. G. Muthu Kumaran, S. Garg, K. Soni, M. Kumar, L.D. Sharma, G. Murali Dhar, K.S. Rama Rao, Ind. Eng. Chem. Res. **46**, 4747 (2007)
33. A.M.A. Naggar, H.M. Gobara, H.A. Sayed, F.S. Soliman, Energy Convs. Manage **106**, 615 (2015)
34. H.H. PhucNguyen, H. Ohkita, T. Mizushima, N. Kakuta, J Jpn Petrol. Inst **54**(6), 373–379 (2011)
35. Z. Cheng, X. Quan, Y. Xiong, L. Yang, Y. Huang, Ultrason. Sonochem. **18**, 1027 (2012)
36. M. Radetic, J. Photochem. Photobiol. C **16**, 62 (2013)
37. S.F. Xiong, Z.L. Yin, Z.F. Yuan, W.B. Yan, W.Y. Yang, Ultrason. Sonochem. **19**, 756 (2012)
38. Y.L. Pang, A.Z. Abdullah, S. Bhatia, Desalination **277**, 1 (2011)
39. N. Talebian, M.R. Nilforoushan, F.J. Mogaddas, Ceram. Int. **39**, 4913 (2013)
40. D. Markovic, B. Jokic, Z. Saponjic, B. Potkonjak, P. Jovancic, M. Radetic, Clean-Soil Air Water **41**(10), 1002 (2013)
41. C.G. Joseph, G.L. Puma, A. Bono, D. Krishnaiah, Ultrason. Sonochem. **16**, 583 (2009)